Journal of Physical Science, Vol. 32(2), 57–70, 2021

Effect of Post-Heating Temperature on Efficiency of Dye-Sensitized Solar Cell with ZnO:Al Thin Films Prepared by Sol-Gel Spin Coating

Nurdin Siregar,* Motlan, and Jonny Haratua Pangabean

Department of Physics, Universitas Negeri Medan, Willem Iskandar Road Pasar V Medan Estate, Medan 20221, Indonesia

*Corresponding author: siregarnurdin@unimed.ac.id

Published online: 25 August 2021

To cite this article: Siregar, N., Motlan, & Pangabean, J. H. (2021). Effect of post-heating temperature on efficiency of dye-sensitized solar cell with ZnO:Al thin films prepared by sol-gel spin coating. *J. Phys. Sci.*, 32(2), 57–70. https://doi.org/10.21315/jps2021.32.2.5

To link to this article: https://doi.org/10.21315/jps2021.32.2.5

ABSTRACT: *Dye-sensitized solar cell (DSSC) has a great potential to convert solar light into electricity. In this article, a prototype of DSSC had been successfully fabricated using ZnO:Al thin film and dye from red dragon fruit as a working electrode. ZnO:Al thin films were prepared by a sol-gel spin coating method with variation of post-heating temperatures. The XRD result confirms that all ZnO:Al thin films have a hexagonal structure with crystal sizes of 16 nm to 41 nm. SEM analysis showed the nanoparticles with particle size of 30 nm to 80 nm. The bandgap ranges from 3.16 eV to 3.40 eV. The EIS analysis reveals that charge transfer resistance greatly decreases with the rise of temperature. The efficiency of DSSC gradually improved with increasing the post-heating temperature. ZnO:Al with a post-heating temperature of 600°C had the highest efficiency of 0.398%.*

Keywords: dye sensitised solar cell, ZnO:Al thin films, sol-gel spin coating, red dragon fruit extract

1. INTRODUCTION

Dye-sensitized solar cell (DSSC) is one of the solar cell types that originally invented by Gratzel in 1991.[1] The fabrication of DSSC is low cost and environmentally friendly. It consists of several components, namely, semiconductor oxide, dye, counter electrode and electrolyte.[2] The engineering of ZnO semiconductor for the DSSC working electrode is promising because it has an energy bandgap of 3.37 eV and a binding energy of 60 meV which allows direct absorption of UV radiation.[3] ZnO thin film has poor electrical characteristic like having a low conductivity value of 6.24×10^{-7} $(\Omega.cm)s^{-1}$.[4] To enhance its physical, optical and electrical properties, it is often doped with extrinsic dopant from group IIIA such as B, Al and Ga as foreign element doped into the ZnO structure.[5] Aluminium (Al) is chosen as a doping agent because it can increase the electrical conductivity of ZnO thin films to an order of 10^5 Ω.cm.[6] There are several techniques to fabricate thin film such as molecular beam epitaxy, radio frequency (RF) magnetron sputtering, pulsed laser deposition, spray pyrolysis, physical vapour deposition, and sol-gel spin coating.[7–12] A sol-gel spin coating method has several advantages, including not using a high vacuum space, low cost, homogeneous composition, controllable layer thickness and great microstructure.[13]

Islam et al. studied Al-doped ZnO and they found that the energy bandgap value was affected by the doping concentrations.[14] The crystal size, transmittance and energy bandgap increase with the increasing of heating temperature.[15] The efficiency of DSSC is not only influenced by Al concentration but also annealing temperature.[16,17] Recently, Bekele et al. had successfully utilised the root extract of *Kniphofia schemperi* as the natural dye for DSSC.[18] Based on these considerations, it is interested to conduct research on DSSC using Al-doped ZnO thin film prepared by a sol-gel spin coating method with variation of post-heating temperatures and extract red dragon fruit as the natural dye sensitized.

2. EXPERIMENTAL

2.1 Synthesis of ZnO:Al Thin Films

ZnO:Al thin film was synthesised using a sol-gel spin coating method.[19] Typically, 4 g of zinc acetate dihydrate and Al 1.0 % was dissolved into 20 ml isopropanol and then stirred with a magnetic stirrer. After 10 min, 1.72 ml diethanolamine (DEA) was added slowly as a stabiliser agent. The gel solution was then dropped onto indium tin oxide (ITO) glass substrate and then rotated by a spin coating with a speed of 5,000 rpm. Finally, the sample was heated with temperature of 250°C for 5 min to remove the excess liquid. Finally, the sample was annealed in an electric furnace with temperatures of 400°C, 450°C, 500°C, 550°C and 600°C for 5 h.

2.2 Characterisations of ZnO:Al Thin Films

The crystal properties of ZnO:Al thin films were evaluated using X-ray diffractometer (LabX XRD-6100, Shimadzu) with Cu K_α radiation (40 kV, 30 mA) of wavelength 1.54 Å. A field emission-scanning electron microscopy (FE-SEM, JEOL 6500) with accelerating voltage of 15 kV and working distance of 10 mm was used to observe the surface morphology of the thin films. The optical properties of thin films were further investigated using UV-visible (UV-vis) spectrometer with both transmission and absorbance modes from the wavelength of 300 nm to 700 nm. Electrochemical impedance spectroscopy was performed using Biologic SP-300 Potentiostat. The characterisations were conducted in Indonesia and Taiwan.

2.3 Preparation of Dye Sensitizer

The extract of dye sensitizer was done by cutting red dragon fruit into small pieces and then put it into a beaker glass. After that, the red dragon fruit is crushed by mortar until smooth. Extraction was done by adding ethanol and then soaked for 24 h in a dark place.[18] Finally, the extract was filtered using filter paper and stored in a under dark place.

2.4 Fabrication of DSSC

The DSSC was fabricated by attaching a platinum counter electrode to a ZnO: Al thin film coated with dye from red dragon fruit which acted as a working electrode with a layer of separating surlyn. Sticking of surlyn was conducted by pressing the working electrode and the counter electrode under heating with temperature of 70°C to 80°C to stick them perfectly.[20] The electrolyte was injected through a small hole found in the counter electrode.

2.5 Efficiency Measurement

Electrical testing was carried out by assembling an electrical circuit between the DSSC and digital multimeters as shown in Figure 1.[21] This test is based on the beam lighting method to determine the performance and efficiency of the cells obtained when the solar cell is exposed to light with a certain intensity at the top anode. DSSC outputs are open-circuit voltage (V_{oc}) and short-circuit current (I_{sc}) DSSC. Then, the fill factor (FF) and the DSSC efficiency (η) were calculated.

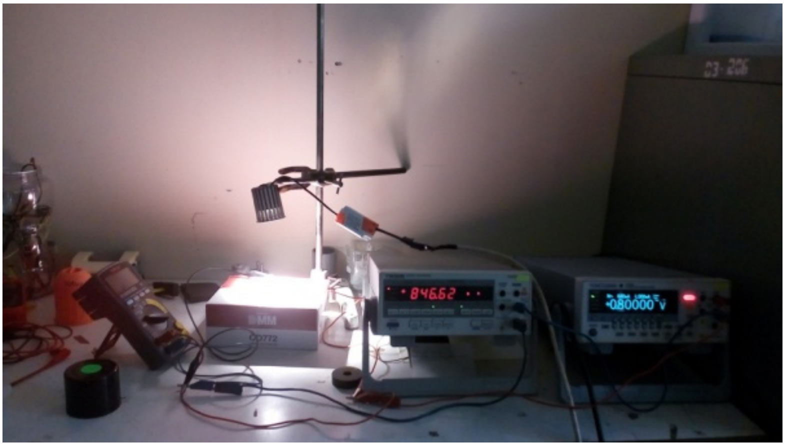

Figure 1: Measurement efficiency of DSSC.

3. RESULTS AND DISCUSSION

3.1 Crystal Structure of ZnO:Al Thin Film

The diffraction pattern of ZnO:Al thin film with variation of post-heating temperatures is shown in Figure 2. The result confirm that all samples have the same crystal structure of hexagonal wurtzite according to the database with JCPDF No. #36-1451.[22] The XRD pattern shows three peaks with (100), (002) and (101) planes where a (101) plane has the highest intensity indicating the preferred crystal growth.

Crystallite size of the samples with variation post-heating temperatures are calculated using the Scherrer's equation.[23]

$$D = \frac{0.9\,\lambda}{\beta \cos\theta} \tag{1}$$

Where, D = crystallite size, λ = wavelength, β = FWHM (full width half maximum), θ = diffraction angle.

Table 1 shows the crystal size increases from 16 nm to 41 nm along with an increase in post-heating temperature from 400°C to 550°C. This was because increasing heating temperature will make compaction increase and grow large granule due to the incorporation of small grains.[24] When the post-heating temperature was increased to 600°C, the crystallite size decreased to 34 nm due to aluminium as dopant block the grain boundaries.[25]

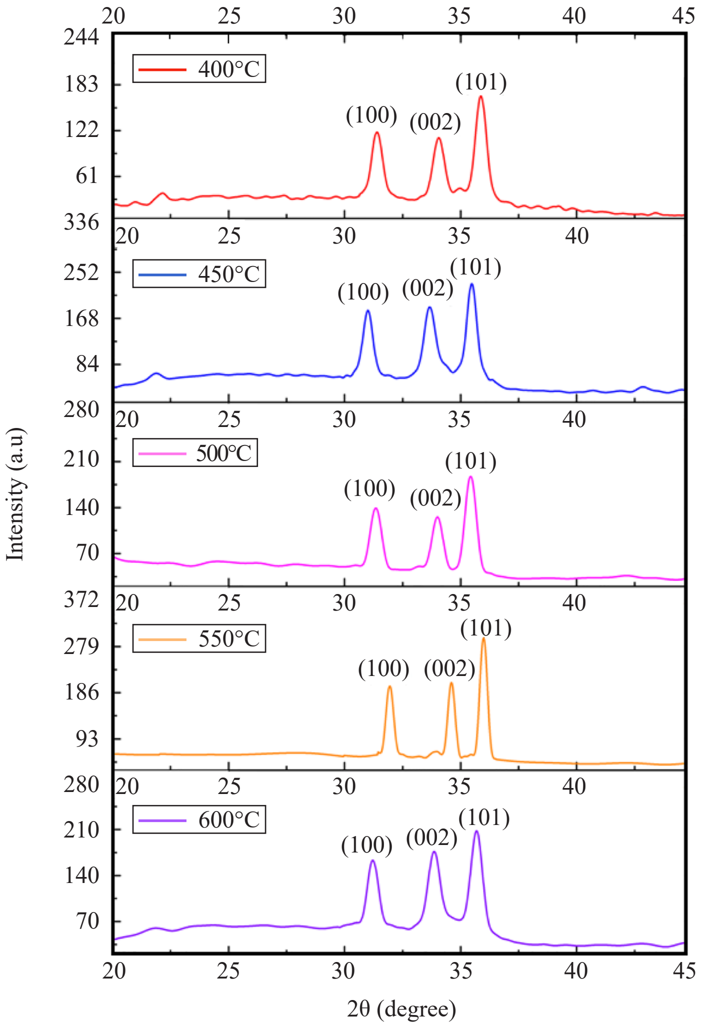

Figure 2: X-ray diffraction spectra of ZnO:Al thin films.

Table 1: Crystal size ZnO:Al thin film with variation post-heating temperatures

Temperature (°C)	Crystal size (nm)
400	16
450	21
500	39
550	41
600	34

3.2 SEM and EDS Analyses of ZnO:Al Thin Film

Figure 3 shows SEM images of ZnO:Al. The surface morphology of thin film contains a lot of tiny nanoparticles with homogenous distribution. It can be seen clearly that there is no obvious different of SEM images for different post-heating temperatures. The SEM images also exhibit that the grains totally cover the substrate without cracking and have a good interconnection between each particle. The average particle size of nanoparticles annealed at 400°C, 500°C and 600°C are 38±7 nm, 50±10 nm and 66±12 nm, respectively. Energy disperse spectroscopy (EDS) analysis was further conducted to confirm the success of Al-doped into ZnO. As shown in Figure 3(d), a representative EDS result exhibits the peak of Al at energy 1.5 KeV with atomic concentration of 0.99%. This analysis confirms that Al as an extrinsic dopant has been successfully doped into ZnO structure. The atomic concentrations of zinc (Zn) and oxygen (O) were 47.13% and 51.88%, respectively.

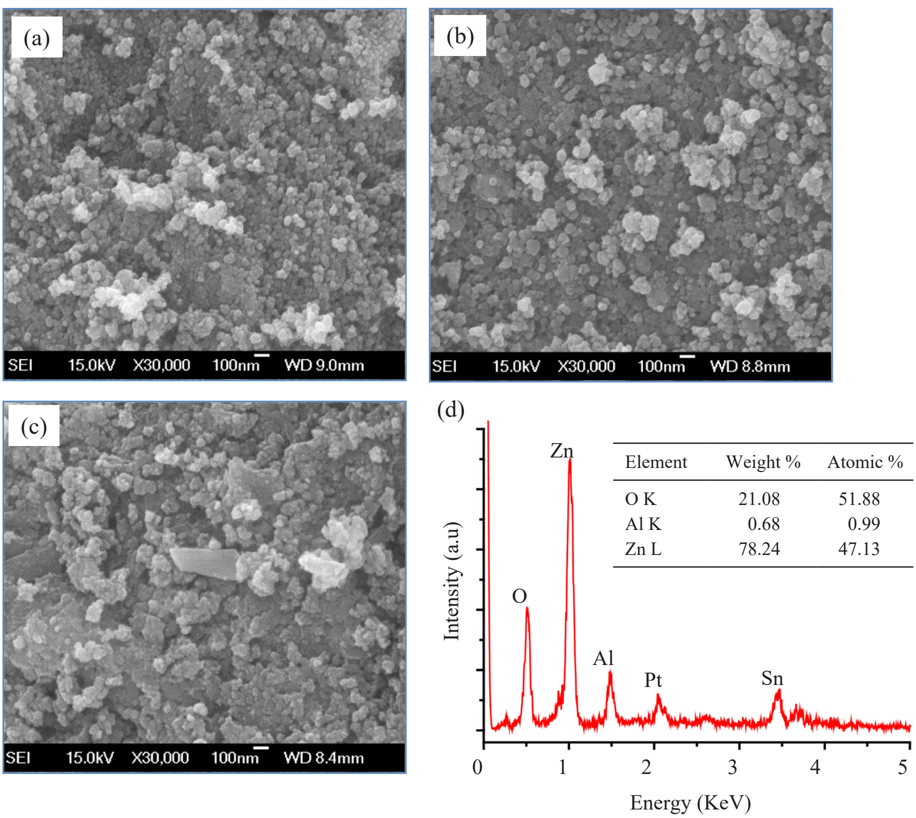

Figure 3: SEM images of ZnO:Al thin films at (a) 400°C, (b) 500°C, (c) 600°C and (d) EDS to show the presence of Al.

3.3 Optical Properties of ZnO:Al Thin Films

Figures 4 and 5 exhibit the transmittance and absorbance spectra, respectively. The transmittance spectrum of the ZnO:Al thin films in Figure 4 shows a sharp increase in the transmittance value for all samples that occurs in the wavelength range of approximately 350 nm to 400 nm, which is the ultraviolet wavelength region. For ZnO:Al thin film samples heated at post-heating temperature, the transmittance value is about 75% to 80% at a wavelength of about 600 nm to 700 nm and the reduction in heating of 500°C. The high transmittance value of thin films is good and suitable for solar cell applications. Figure 5 shows the absorbance edges of the samples heated at temperatures of 450°C and 550°C shift to a shorter wavelength region, while those of samples heated at post-heating temperatures of 500°C and 600°C shift to a longer wavelength region.

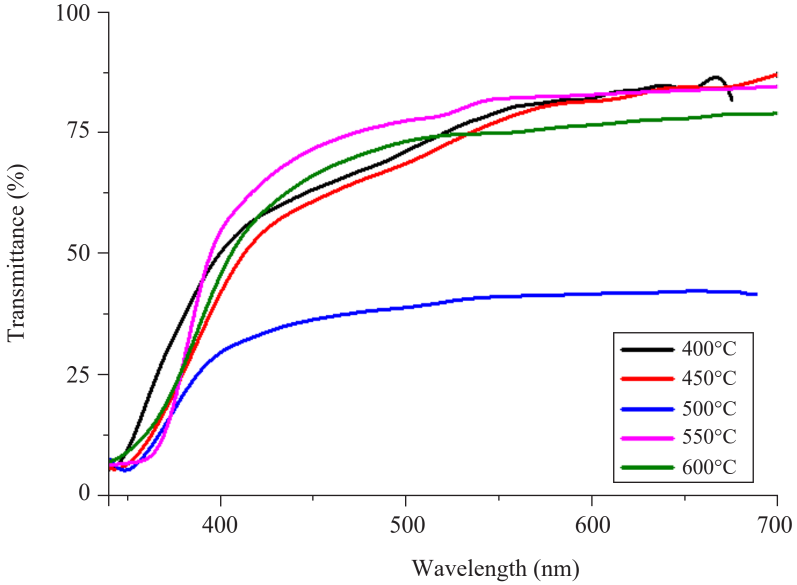

Figure 4: Transmittance spectrum of ZnO:Al thin films.

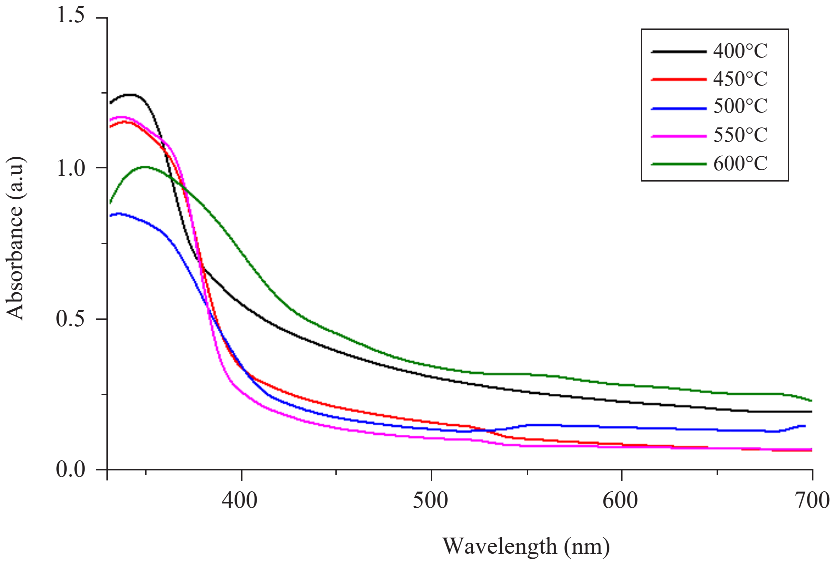

Figure 5: Absorbance spectrum of ZnO:Al thin films.

The energy bandgap of the ZnO:Al thin film is further calculated using Equation 2.[26]

$$(\alpha hv)^2 = C_D\,(hv - E_{opt}) \tag{2}$$

Where, α = absorption coefficient, v = frequency, C_D = proportionality constant, h = Planck's constant and E_{opt} = optical bandgap.

Based on the Tauc Plot method in Figure 6, the energy bandgap of the ZnO:Al thin films with variation post-heating temperatures could be obtained. Table 2 lists that the energy bandgap value increases from 3.16 eV to 3.40 eV with increasing the post-heating temperature from 400°C to 500°C. When the post-heating temperature was increased to 550°C and 600°C, the energy bandgap value slightly decreased to 3.20 eV. This phenomenon may be related to defects in thin film due to rise of heating temperature.[27]

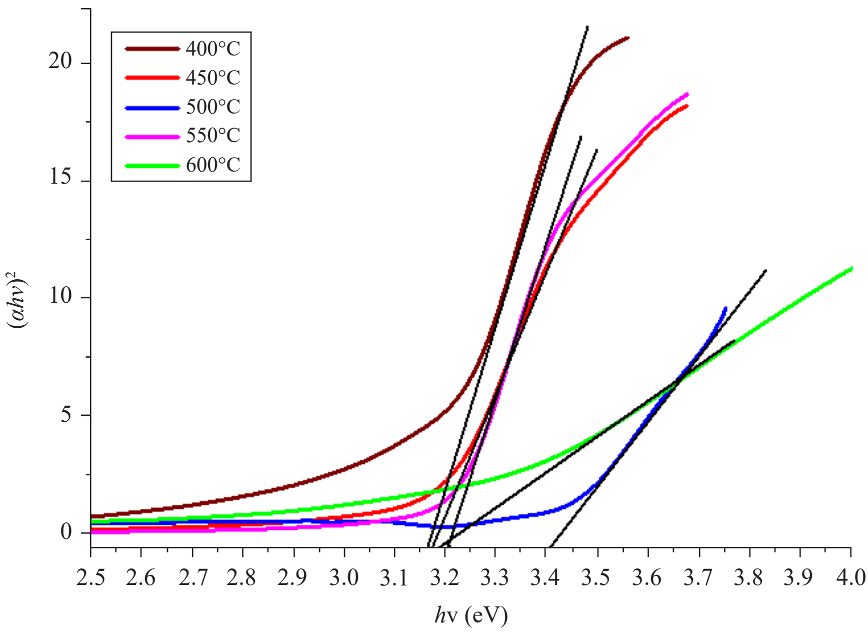

Figure 6: Energy bandgap of ZnO:Al thin films using Tauc Plot.

Table 2: Energy bandgap of ZnO:Al thin films.

Temperature (°C)	Bandgap (eV)
400	3.16
450	3.17
500	3.40
550	3.20
600	3.20

3.4 Dye Spectrum of Red Dragon Fruit Extract

The absorbance spectrum of red dragon fruit solution was tested with UV-vis spectrophotometer. Figure 7 shows that the red dragon fruit dye has the absorbance at UV and visible light range with peak absorbance of 254 nm and 570 nm, respectively. The result indicates that the extract of red dragon fruit has a great potential to be used as the dye sensitizer for DSSC device.

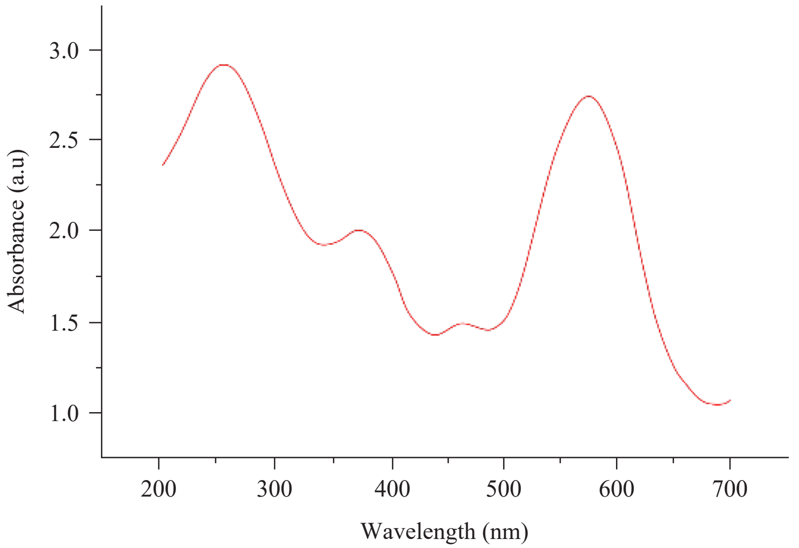

Figure 7: Absorbance of red dragon fruit dye.

3.5 DSSC Efficiency

The DSSC efficiency can be obtained by comparing the power produced by the prototype DSSC with the power of light source (P_{in}), as shown in Equations 3 and 4.

$$\eta = \frac{P_{max}}{P_{in}} \times 100\% = FF \frac{J_{SC} \times V_{OC}}{P_{in}} \times 100\% \qquad (3)$$

$$FF = \frac{J_{max} \times V_{max}}{J_{SC} \times V_{OC}} \qquad (4)$$

Where, η = DSSC efficiency (%), J_{sc} = current density (mA), V_{oc} = voltage (mV), P_{in} = input power (mW) and FF = fill factor.

As listed in Table 3, the efficiency of DSSC increases with the rise of post-heating temperature. The maximum efficiency is 0.398% at a temperature of 600°C. The reasons for this could be explained: first, a better crystallinity as proved by XRD analysis; and second, the absorption spectra in Figure 5 exhibits that ZnO:Al with annealing temperature of 600°C had the highest absorption in the visible light region among other temperatures. To further investigate the higher efficiency with a higher temperature, the electrochemical impedance spectra (EIS) analysis was conducted in electrolyte solution of potassium chloride (KCl, 1M). The EIS data can be used to evaluate the charge transfer property by comparing the diameter of that semicircle in Figure 8. The charge transfer resistance (R_{ct}) could be determined after fitting technique. The value of R_{ct} for heating at 600°C is 6.5 kΩ, which is lower than at 500°C (7.6 kΩ) or 400°C (9.5 kΩ). Therefore, the other reason for maximum efficiency at 600°C post-heating temperature is due to its lowest resistance that leading to most efficient charge transfer. We realised that presence efficiency is still relatively low but there is always room for improvement. Therefore, further research and development is needed to conduct in the future.

Table 3: Values of voltage, current density, power, fill factor and efficiency of DSSC.

Temperature (°C)	V_{oc} (V)	J_{sc} (mA/cm^2)	P_{max} (W/cm^2)	FF (%)	η (%)
400	0.45	0.350	0.031	19.644	0.084
450	0.45	0.450	0.052	25.925	0.143
500	0.45	0.487	0.068	31.339	0.188
550	0.50	0.650	0.094	28.941	0.257
600	0.55	1.168	0.250	22.605	0.398

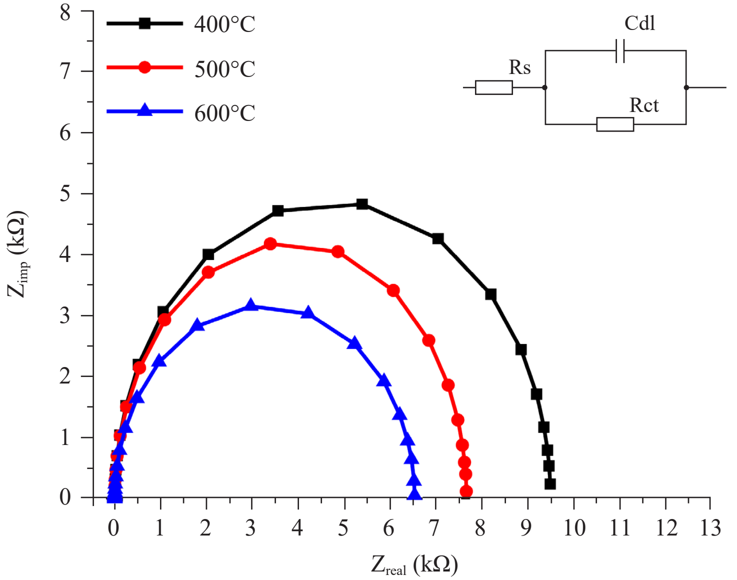

Figure 8: EIS of ZnO:Al thin films.

4. CONCLUSION

The DSSC prototype has been successfully fabricated using ZnO:Al thin film and dye from red dragon fruit extract as working electrodes. The XRD analysis confirmed that all samples had the hexagonal wurtzite structure. The bandgap values of thin films were about of 3.16 eV to 3.40 eV. The surface morphology of ZnO:Al thin films was nanoparticle with particle size less than 100 nm. We found that the efficiency of DSCC gradually improved with increasing the post-heating temperature. ZnO:Al with post-heating temperature of 600°C had the highest efficiency of 0.398%. The optimum efficiency was contributed by the better crystallinity, more efficient charge transfer and higher absorption properties.

5. ACKNOWLEDGEMENTS

This work was supported by the Indonesia Directorate of Research and Community Service (No. 027/UN33.8/LL/2018).

6. REFERENCES

1. Grätzel, M. (1998). Demonstrating electron transfer and nanotechnology: A natural dye-sensitized nanocrystalline energy converter. *J. Chem. Educ.*, 75(6), 752. https://doi.org/10.1021/ed075p752
2. Vittal, R. & Ho, C. K. (2017). Zinc oxide based dye-sensitized solar cells: A review. *Renew. Sustain. Energy Rev.*, 70, 920–935. https://doi.org/10.1016/j.rser.2016.11.273
3. Siregar, N., Motlan & Panggabean, J. H. (2020). The effect magnesium (Mg) on structural and optical properties of ZnO:Mg thin film by sol-gel spin coating method. *J. Phys. Conf. Ser.*, 1428(012026). https://doi.org/10.1088/1742-6596/1428/1/012026
4. Zhai, C.-H. et al. (2016). Effects of Al doping on the properties of ZnO thin films deposited by atomic layer deposition. *Nanoscale Res. Lett.*, 11, 407. https://doi.org/10.1186/s11671-016-1625-0
5. Tumbul, A. et al. (2018). Solution processed boron doped ZnO thin films: Influence of different boron complexes. *Mater. Res. Express*, 6(3), 035903. https://doi.org/10.1088/2053-1591/aaf4d8
6. Amara, S. & Bouafia, M. (2015). Investigation on optical, structural and electrical properties of annealed AZO/Al/AZO multilayer structures deposited by dc magnetron sputtering. *J. Mater. Sci. Mater. Electron.*, 26(3), 1763–1769. https://doi.org/10.1007/s10854-014-2605-8
7. Opel, M. et al., (2013). Laser molecular beam epitaxy of ZnO thin films and heterostructures. *J. Phys. D: Appl. Phys.*, 47(3), 034002. https://doi.org/10.1088/0022-3727/47/3/034002

8. Dave, P. Y. et al. (2016). Examination of zinc oxide films prepared by magnetron sputtering. *Procedia Tech.*, 23, 328–335. https://doi.org/10.1016/j.protcy.2016.03.034
9. Wang, Z. et al. (2019). Vacancy cluster in ZnO films grown by pulsed laser deposition. *Sci. Rep.*, 9, 3534. https://doi.org/10.1038/s41598-019-40029-3
10. Cho, J. et al. (2019). Transparent ZnO thin-film deposition by spray pyrolysis for high-performance metal-oxide field-effect transistors. *Materials*, 12(20), 3423. https://doi.org/10.3390/ma12203423
11. Jouya, M., Taromian, F. & Siami, S. (2017). Rapid growth of zinc oxide nanobars in presence of electric field by physical vapor deposition. *J. Theor. Appl. Phys.*, 11, 291–299. https://doi.org/10.1007/s40094-017-0270-z
12. Yadav, A. B., Pandey, A. & Jit, S. (2014). Effects of annealing temperature on the structural, optical, and electrical properties of ZnO thin films grown on n-Si ⟨100⟩ substrates by the sol-gel spin coating method. *Acta. Metall. Sin. (English Lett.)*, 27, 682–688. https://doi.org/10.1007/s40195-014-0097-4
13. Hosseinnejad, M. T. et al. (2016). Preparation of nanostructured ZnO thin films using magnetron sputtering for the gas sensors applications. *J. Inorg. Organomet. Polym.*, 26, 405–412. https://doi.org/10.1007/s10904-015-0324-0
14. Islam, M. R. et al. (2019). Structural, optical and photocatalysis properties of sol-gel deposited Al-doped ZnO thin films. *Surf. and Interfaces*, 16, 120–126. https://doi.org/10.1016/j.surfin.2019.05.007
15. Chen, W.-J. et al. (2012). Synthesis of ZnO:Al transparent conductive thin films using sol-gel method. *Procedia Eng.*, 36, 54–61. https://doi.org/10.1016/j.proeng.2012.03.010
16. Chou, J.-C. et al. (2019). Dye-sensitized solar cells using aluminum-doped zinc oxide/titanium dioxide photoanodes in parallel. *Energies*, 12(18), 3469. https://doi.org/10.3390/en12183469
17. Pandey, P. et al. (2017). Effects of annealing temperature optimization on the efficiency of ZnO nanoparticles photoanode based dye sensitized solar cells. *J Mater Sci: Mater Electron*, 28, 1537–1545. https://doi.org/10.1007/s10854-016-5693-9
18. Bekele, E.T. et al. (2021). Biotemplated synthesis of titanium oxide nanoparticles in the presence of root extract of Kniphofia schemperi and its application for dye sensitized solar cells. *Int. J. Photoenergy*, 2021, 6648325. https://doi.org/10.1155/2021/6648325
19. Siregar, N., Motlan & Panggabean, J. (2020). The effect magnesium (Mg) on structural and optical properties of ZnO:Mg thin film by sol-gel spin coating method. *J. Phys. Conf. Ser.*, 1428, 012026. https://doi.org/10.1088/1742-6596/1428/1/012026
20. Kumar, R., Sahajwalla, V. & Bhargava, P. (2019). Fabrication of a counter electrode for dye-sensitized solar cells (DSSCs) using a carbon material produced with the organic ligand 2-methyl-8-hydroxyquinolinol (Mq). *Nanoscale Adv.*, 1(8), 3192–3199. https://doi.org/10.1039/C9NA00206E

21. Motlan & Siregar, N. (2018). The effect of post-heating temperature on of the eficency of dye sensitized solar cell (DSSC) with using ZnO thin film and dye from Dutch eggplant fruit (*Solanum betaceum*). *J. Phys. Conf. Ser.*, 1120, 012082. https:// /doi.org/10.1088/1742-6596/1120/1/012082
22. Gultom, N. S., Abdullah, H. & Kuo, D.-H. (2020). Phase transformation of bimetal zinc nickel oxide to oxysulfide photocatalyst with its exceptional performance to evolve hydrogen. *Appl. Catal. B.*, 272, 118985. https://doi.org/10.1016/j.apcatb.2020.118985
23. Gultom, N. S., Abdullah, H. & Kuo, D.-H. (2019). Facile synthesis of cobalt-doped (Zn,Ni)(O,S) as an efficient photocatalyst for hydrogen production. *J. Energy Inst.*, 92(5),1428–1439. https://doi.org/10.1016/j.joei.2018.08.008
24. Mohammadi, M., Roknabadi, M. R. & Arabshahi, H. (2010). Investigations on impact of post-heat temperatures, optical and electrical properties of Al-doped ZnO thin films prepared by sol-gel method. *Indian J. Sci. Technol.*, 3(2), 110–112. https://doi.org/10.17485/ijst/2010/v3i2/29659
25. Darvishi Kamachali, R. (2020). A model for grain boundary thermodynamics. *RSC Adv.*, 10(45), 26728–26741. https://doi.org/10.1039/D0RA04682E
26. Abdullah, H. et al. (2020). Effects of tin in La–Sn-Codoped Zn(O,S) photocatalyst to strongly cleave the Azo bond in Azobenzene with in situ generated hydrogen. *ACS ACS Appl. Mater. Interfaces.*, 12(14), 16186–16199. https://doi.org/10.1021/acsami.9b19885
27. Sengupta, J., Ahmed, A. & Labar, R. (2013). Structural and optical properties of post annealed Mg doped ZnO thin films deposited by the sol-gel method. *Mater. Lett.*, 109, 265–268, https://doi.org/10.1016/j.matlet.2013.07.104